ISSN 1027-5495. Functional Materials, 23, No.1 (2016), p. 32-39.
doi:http://dx.doi.org/10.15407/fm23.01.032 © 2016 — STC "Institute for Single Crystals"

# Structural and microstructural properties of $Cd_{1-x}Zn_xTe$ films deposited by close spaced vacuum sublimation

***Y.V.Znamenshchykov*[1], *V.V.Kosyak*[1], *A.S.Opanasyuk*[1], *M.M.Kolesnyk*[1], *V.V.Grinenko*[1], *P.M.Fochuk*[2]**

[1]Sumy State University, 2 Rymskogo-Korsakova Str., 40007 Sumy, Ukraine
[2]Y.Fedkovych Chernivtsi National University, 2 Kotsjubynskyi Str., 58012 Chernivtsi, Ukraine

*Received September 9, 2015*

The structural properties (microstresses, texture, lattice parameter, coherent scattering domains size) and chemical composition of $Cd_{1-x}Zn_xTe$ (CZT) films with variable zinc concentration were studied. Films were deposited on molybdenum coated glass substrates by close spaced vacuum sublimation method. Properties of samples were investigated by X-ray diffraction, energy dispersive spectroscopy, scanning electron microscopy. Zinc concentration in CdZnTe layers was determined by the EDS and from the lattice parameter, according to the literature data. Namely, it was determined that the CZT films had following Zn concentrations: $x = 0.09$, $x = 0.24$, $x = 0.30$.
**Keywords**: Composition of $Cd_{1-x}Zn_xTe$, microstresses, texture, lattice parameter, coherent scattering domains size.

Исследованы структурные свойства (микронапряжения, текстура, период решетки, размер областей когерентного рассеивания) и химический состав пленок $Cd_{1-x}Zn_xTe$ (CZT) с переменной концентрацией цинка. Слои получены методом термического испарения в квазизамкнутом объеме на подложках из стекла, покрытого молибденом. Свойства пленок исследованы с помощью методов рентгеновской дифрактометрии, энергодисперсной спектроскопии, сканирующей электронной микроскопии. Концентрация цинка в слоях CdZnTe определена по результатам EDS и значению параметра кристаллической решетки материала, в соответствии с литературными данными. Установлено, что слои CZT имели концентрации цинка: $x = 0.09$, $x = 0.24$, $x = 0.30$.

**Структурні та субструктурні властивості плівок Cd1-xZnxTe, отриманих методом вакуумного термічного випаровування в квазізамкненому об'ємі.** *Я.В.Знаменщиков, В.В.Косяк, А.С.Опанасюк, М.М.Колесник, В.В.Гриненко, П.М.Фочук.*

Досліджено структурні властивості (мікронапруження, текстура, період гратки, розмір областей когерентного розсіювання) та хімічний склад плівок $Cd_{1-x}Zn_xTe$ (CZT) зі змінною концентрацією цинку. Шари отримано методом термічного випаровування у квазізамкненому об'ємі на підкладках зі скла, покритого молібденом. Властивості плівок досліджено за допомогою методів рентгенівської дифрактометрії, енергодисперсної спектроскопії, скануючої електронної мікроскопії. Концентрацію цинку в шарах CdZnTe визначено за результатами EDS та значеннями параметра кристалічної гратки матеріалу, відповідно до літературних даних. Встановлено, що шари CZT мають концентрації цинку: $x = 0.09$, $x = 0.24$, $x = 0.30$.

## 1. Introduction

Cadmium telluride (CdTe), zinc telluride (ZnTe) compounds and their solid solutions (CZT) attract considerable interest because of their wide application in optoelectronics, microelectronics, sensor electronics, and photovoltaic [1, 2]. These compounds and their solid solutions are promising photorefractive materials for optical memory devices and information processing systems [3, 4]. Also CZT is used in fabrication of photodetectors, solar cells, radiation detectors, filters for visible and ultraviolet radiation, etc. [5, 6].

CZT solid solution has a number of advantages over CdTe in development of the high efficiency X-ray and gamma-ray detectors [7, 8]. This is due to high resistivity of the material, higher atomic binding energy than in CdTe, ability to vary band gap of the material in the range from $E_g = 1.46$ eV (CdTe) to $E_g = 2.26$ eV (ZnTe) [1, 9]. Also CZT films with Zn concentration of $x = 0.3$, which has band gap of about 1.70 eV, are important materials for top absorbing layer of the first element of tandem solar cells [10]. Structural properties of CZT single crystals are well-studied [11]. Whereas, films of this material obtained by vacuum methods, are not investigated well because of difficulties in their deposition. In particular, evaporation of II–VI compounds occurs with dissociation, and partial pressures of the components are quite different. At the same time for application in electronic devices, especially for fabrication of radiation detectors, the CZT layers with big grain size, quality texture, low concentration of dislocations and stacking faults, controllable electrical and optical properties are required. However, it is difficult to obtain layers with such a properties by the low-cost methods for example electrodeposition, thermal vacuum evaporation, since these techniques do not provide equilibrium conditions for the films growth.

The goal of this work was to study the effect of zinc concentration on structural properties of the CZT films, obtained by CSVS method, which allows to perform evaporation in grown conditions close to thermodynamic equilibrium. Also comparison of structural properties and phase composition of the CZT solid solutions and pure CdTe and ZnTe compounds films was performed.

## 2. Experimental details

CdTe, ZnTe and CZT solid solutions films were deposited on molybdenum coated glass substrates by (CSVS) method in VUP-5M vacuum equipment, residual gas pressure in a chamber did not exceed of $5 \cdot 10^{-5}$ Pa.

In order to obtain the CZT films, co-evaporation of CdTe and ZnTe powder was performed. For this purpose we have developed system for co-evaporation, which is based on system used in our previous works [12, 13] for CdTe deposition. It was equipped with two independent evaporators for CdTe and ZnTe. Weight of cadmium telluride powder was 60 mg, weight of evaporated zinc telluride powder was varied from the film to film correspondently — 10 mg (CZT1), 20 mg (CZT2), 30 mg (CZT3).

Surface morphology of the films was investigated by scanning electron microscope (SEM-102E). The average grain size ($D$) in the layers was estimated by the Jeffries method.

Chemical composition of the films was studied by EDS. Determination of the mass concentration of the compound components was carried out in the area of 200×200 μm (beam exposure — 100 sec, sensitivity — 1000 imp/sec, beam energy — 20 keV) on the samples surface. It should be noted that the samples surface was not etched or polished for more precise EDS measurements, and the film surface was assumed to be flat. However roughness of the film could lead qto some increasing in error of quantitative EDS analysis [14]. For quantitative EDS analysis we used database of reference chemical elements of the "Invent" company (Moscow, Russia).

X-ray diffraction analysis was used to study the structural properties of the layers. Measurements of XRD spectra was carried out by DRON4-07 equipment with a conventional Bragg-Brentano θ–2θ geometry (2θ is the Bragg's angle) using Ni-filtered $CuK_\alpha$ radiation ($\lambda = 0.15406$ nm, $U = 40$ kV, $I = 40$ mA). The samples were measured in the 2θ angle range from 20 to 80°.

The peak intensities were normalized to the intensity of (111) peak of the cubic phase. Phase analysis was performed by comparison of the inter-planar distances as well as relative intensities measured from the samples and reference of the Joint Committee on Powder Diffraction Standards (JCPDS card No. 15-0770) data [15].

Texture of the films was determined by the Harris method [13, 16]. The pole density was calculated as:

$$P_i = \frac{(I_i/I_{0i})}{\frac{1}{N}\sum_{i=1}^{N}(I_i/I_{0i})}, \qquad (1)$$

where $I_i$, $I_{0i}$ — are the integral intensities of $i$-diffraction peak for the film and reference powder sample of CdTe, respectively, $N$ is a number of lines observed in the XRD pattern.

Texture axis has those indices that correspond to the maximum value of $P_i$. In this case, the orientation factor can be found from the expression

$$f = \sqrt{\frac{1}{N}\sum_{i=1}^{N}(P_i - 1)^2}. \qquad (2)$$

Calculation of the cubic phase lattice constant a was carried out using the following formula:

$$a = \frac{\lambda}{2\sin\theta}\sqrt{(h^2 + k^2 + l^2)}. \qquad (3)$$

Precise values of the lattice parameter were determined by the extrapolated Nelson-Riley method [17]. For this purpose, dependences were plotted in $a(c)$ and $1/2\cos2\theta(1/\sin(\theta) + 1/\theta)$ coordinates.

The XRD method was also applied for determination of average size $L$ of the coherent scattering domains (CSD) and microstrain level $\varepsilon$ from broadening of the diffraction peaks.

The average coherent scattering domains size was determined from the Debye-Scherrer formula [18]:

$$L = \frac{k \cdot \lambda}{\beta \cdot \cos\theta}, \qquad (4)$$

where $k$ is the constant approximately equal to unity and related to crystallite shape ($k = 0.9$), $\beta$ is the physical broadening of corresponding diffraction peaks.

Microstrain level $\varepsilon$ was calculated using formula [19]:

$$\varepsilon = \frac{\beta \cdot \cos\theta}{4}. \qquad (5)$$

The Cauchy and Gauss approximations were used to separate diffraction broadening due to physical effects and instrumental broadening. In order to separate the contributions in the physical broadening from the dispersive structure of the polycrystalline films and microstrain level the Hall approximation was applied [13].

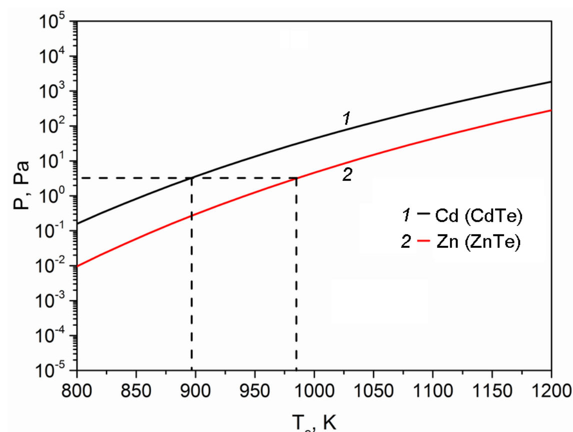


Fig. 1. Dependences of partial pressures of Cd, Zn from evaporator temperature. Dashed lines show temperatures at which the partial pressures of Cd over CdTe (*1*) and Zn over ZnTe (*2*) are equal.

### 3. Results and discusiion

Since we used co-evaporation of CdTe and ZnTe powders from two independent sources, it was necessary to determine temperatures of CdTe and ZnTe evaporators, which provide the optimal conditions for deposition of the CZT films.

Our previous studies suggest the following optimal temperature for the deposition of CdTe and ZnTe films: CdTe evaporator temperature $T_{e(CdTe)} = 893$ K [13, 18], ZnTe evaporator temperature $T_{e(ZnTe)} = 993$ K [18] and the substrate emperature $T_s = 693$ K. Such growth conditions allow to obtain the highly textured single-phase films of CdTe and ZnTe compounds with the low microstrain level, low concentrations of packing defects and dislocations, which are suitable for application in the electronic devices.

It is well known, that difficulty in obtaining of the CZT solid solution films by vacuum methods is related to incongruent evaporation of CdTe and ZnTe compounds. Process of evaporation can be described by formula [20]:

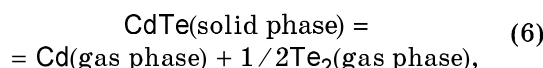

$$CdTe(\text{solid phase}) = Cd(\text{gas phase}) + 1/2Te_2(\text{gas phase}), \qquad (6)$$

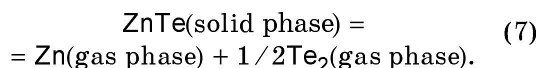

$$ZnTe(\text{solid phase}) = Zn(\text{gas phase}) + 1/2Te_2(\text{gas phase}). \qquad (7)$$

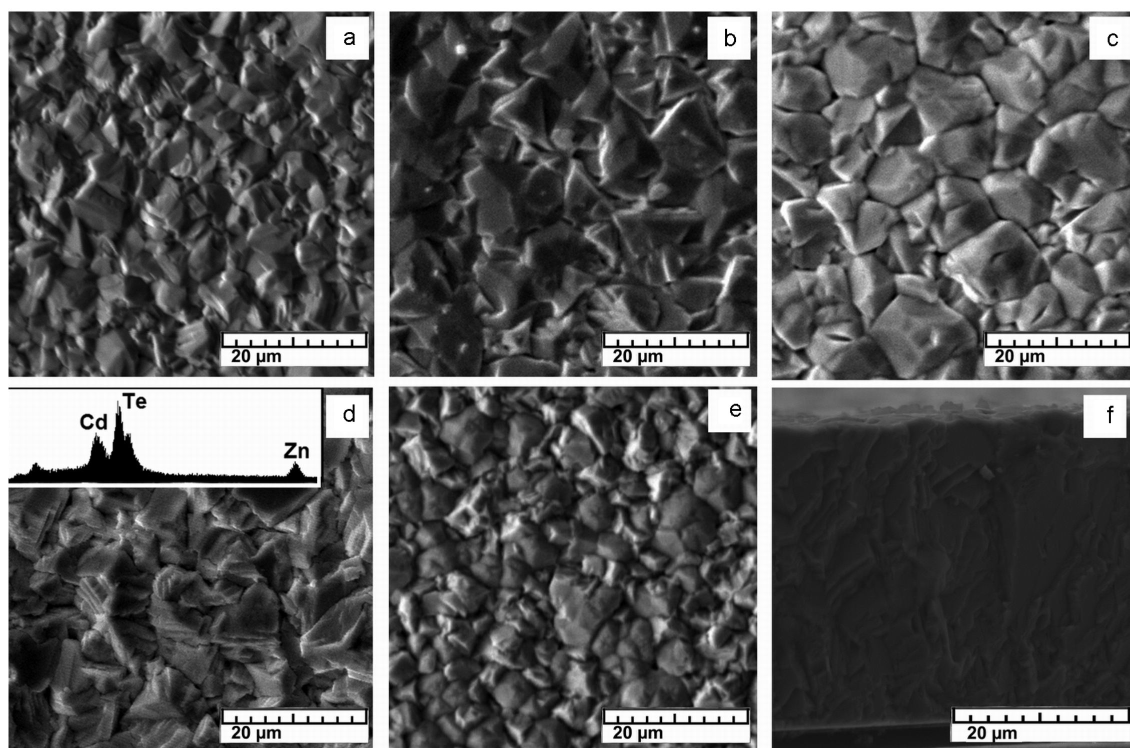


Fig. 2. SEM images of surface of CZT films with different zinc concentration: $x = 0$ (CdTe) (a); $x = 0.09$ (b); $x = 0.24$ (c); $x = 0.30$ (d); $x = 1$ (ZnTe) (e), and film cross-section of film with Zn concentration $x = 0.30$ (f). In the inset the EDS spectrum of CZT film is presented.

As a result the gas phase contains Cd and Zn atoms as well as $Te_2$ molecules. It should be noted that the pressures of saturated vapor of Cd and Zn have significant differences at the same evaporation temperature. Thus it was necessary to find the evaporating temperatures of compounds at which partial vapor pressures are equal. Calculation of the partial pressures for the components was carried out using equations [20]:

$$\log P_{\mathrm{Te}_2} = -\frac{A}{T} + B, \quad (8)$$

$$P_{\mathrm{Cd(Zn)}} = 2 \cdot P_{\mathrm{Te}_2}, \quad (9)$$

where $P$ — pressure (atm.), $A$, $B$ — the coefficients (CdTe: $A = 9761$ K, $B = 6.57$; ZnTe: $A = 10723$ K; $B = 6.556$), $T$ — temperature (K). The coefficients $A$ and $B$ were taken from the literature [21].

Results of the calculation of temperature dependence of partial pressures of Cd and Zn, formed as a result of dissociation of CdTe and ZnTe compounds during the evaporation, are shown in Fig. 1. Using these dependences it is possible to find the evaporation temperatures of CdTe and ZnTe at which values of the partial vapor pressures of Zn and Cd will be equal. At that, the temperatures of substrate and evaporator must be close to the optimal values determined for pure CdTe and ZnTe, as it was mentioned above.

As it can be seen from Fig. 1, the partial pressures of Cd and Zn are equal and have a value of about 4 Pa at temperatures of CdTe and ZnTe evaporators of 893 and 983 K, correspondently. Comparison of the selected temperatures with the above mentioned optimal temperatures for deposition of CdTe and ZnTe films indicates that selected temperature $T_{e(CdTe)} = 893$ K of CdTe evaporator is equal to the optimal for evaporation of CdTe and temperature of ZnTe evaporator $T_{e(ZnTe)} = 983$ K is close to the optimal for evaporation of ZnTe (993 K). Thus, these temperatures were chosen for the co-evaporation of CdTe and ZnTe powder to obtain the CZT solid solution films.

SEM images of the films surface are shown in Fig. 2. As follows from Fig. 2 the average grain size is changed from 5 to 3.5 µm with increasing of Zn concentration. Also it was determined from the SEM photo of the film cross-section (Fig. 2f), that the grains have columnar-like structure similar

Table 1. Lattice parameter of films and concentration of components

| Sample | Zn($x$) according to EDS | Lattice parameter $a$, nm | Zn($x$) according to lattice parameter | | | |
|---|---|---|---|---|---|---|
| | | | Berchenko [25] | Ramalingam [26] | Vegard (JCPDS) [15, 24] | Our data |
| CdTe | 0 | 0.64947 | 0 | 0 | 0 | 0 |
| CZT1 | 0.09 | 0.64465 | 0.09 | 0.095 | 0.090 | 0.11 |
| CZT2 | 0.24 | 0.64043 | 0.18 | 0.200 | 0.205 | 0.22 |
| CZT3 | 0.30 | 0.63626 | 0.29 | 0.305 | 0.315 | 0.33 |
| ZnTe | 1 | 0.61233 | 1 | 1 | 1 | 1 |

to pure CdTe and ZnTe [13, 22], and the film thickness is 22–29 μm.

Typical EDS spectrum of the layer is shown in the inset of Fig. 2d Analysis of the spectra shows that the film contains only components of the solid solution — Cd, Zn, Te. Scanning of the films surfaces reveals homogeneous composition in the whole area. The obtained spectra were used for determination of atomic concentration of the layers components. According to the EDS data, the films have the following zinc concentrations: $x = 0$ (CdTe film), Ix = 0.09 (CZT1 film), $x = 0.24$ (CZT2 film), $x = 0.30$ (CZT3 film), and $x = 1$ (ZnTe film).

The XRD patterns of the films are presented in Fig. 3. As it is seen from Fig. 3 with increasing of Zn concentration the diffraction peaks are shifting towards the higher values of diffraction angles.

Phase analysis was carried out using JCPDS reference (card 15-0770). As follows from Fig. 3, peak at 24.10°–24.60° angles which corresponds to the reflection from (111) plane of the cubic phase CdTe, ZnTe, CZT is dominant. Also peaks from (220), (311), (400), (422), (511) planes of the cubic zincblende phase are detected on the XRD spectra. The peaks of other phases such as hexagonal phase of CZT were not observed. However, the low intensity peaks on the XRD patterns of CZT1 (at 32°) and CZT3 (at 37° and 43°) films, which are not correspond to the cubic phase of CdZnTe, are observed. Possibly these peaks belong to the copper film, which was deposited on the side of the sample as current collecting contact for the SEM analysis.

The peak splitting observed on the XRD patterns of CZT2 and CZT3 films indicates the presence of a number of solid solutions with different, but similar, zinc concentrations. In order to identify these solid solutions the separation and simulation of the peaks were carried out. For example, in

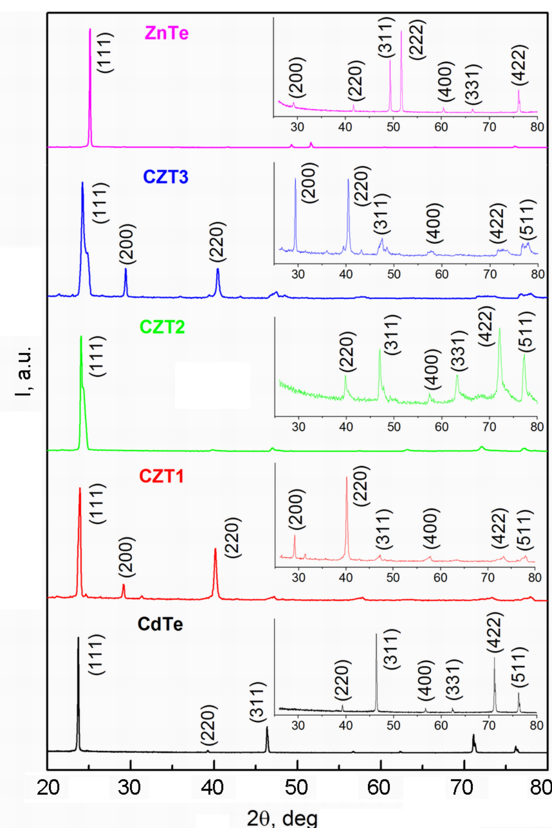


Fig. 3. XRD patterns of CZT films with different zinc concentration. In the inset the position of diffraction peaks on a larger scale is shown (except [111]).

both cases, (111) peak was separated into the peak with higher intensity and the peak with significantly smaller intensity. To perform calculation of the structural and microstructural properties we used peak with higher intensity.

Lattice parameters of the CZT solid solution are very sensitive to the presence of zinc atoms because of deformation of the crystal [23]. That is why we carried out determination of the lattice parameter of

Table 2. Dependences of pole density $P_i$ on angle φ between texture axis and normal to the reflection plane.

| Sample | Zn($x$) | $f$, a.u. | Pole density, $P_i$, arb. units | | | | | | |
|---|---|---|---|---|---|---|---|---|---|
| | | | (111) φ = 0.00 | (422) φ = 19.47 | (331) φ = 22.00 | (311) φ = 29.50 | (220) φ = 35.27 | (511) φ = 38.94 | (400) φ = 54.74 |
| CdTe | 0 | 0.80 | 1.33 | 2.15 | 0.19 | 1.02 | 0.05 | 1.97 | 0.30 |
| CZT1 | 0.09 | 0.71 | 1.98 | 0.61 | 0.01 | 0.22 | 1.54 | 1.70 | 0.94 |
| CZT2 | 0.24 | 0.97 | 2.87 | 1.18 | 0.45 | 0.28 | 0.07 | 1.89 | 0.27 |
| CZT3 | 0.30 | 0.79 | 2.17 | 0.48 | 0.17 | 0.42 | 0.93 | 2.24 | 0.59 |
| ZnTe | 1 | 1.72 | 4.72 | 0.59 | 0.08 | 0.38 | 0.03 | – | 0.19 |

the films according to the Nelson-Riley method, the results of calculation are listed in Table 1. As follows from Table 1 the lattice parameter of the CZT films is decrease with increasing of Zn concentration, which corresponds with the literature data.

For the further determination of zinc concentration we used the Vegard's law which describes relationship between Zn concentration and lattice parameter:

$$d(Cd_{1-x}Zn_xTe) = d(ZnTe) + (1-x)[d(CdTe) - d(ZnTe)], \quad (10)$$

where $d$(CdTe) and $d$(ZnTe) — lattice parameters of CdTe and ZnTe respectively, $x$ — value of Zn concentration.

It should be noted that using of different reference data of $d$(CdTe) and $d$(ZnTe) lead to different compositional dependencies of CZT lattice parameter $a$.

As values of the lattice parameters of pure compounds we used the reference data for CdTe and ZnTe single crystals (Fig. 4 line 3) [15, 24] and results obtained in this work (Fig. 4 line 4). In addition to Eq. (10) we used concentration dependencies of the lattice parameter of solid solutions which were experimentally found in the works [25, 26] by Berchenko and Ramalingam (Fig. 4 lines 1–2).

Analysis of $a$–$x$ dependences in [25, 26] indicates that there is some difference between real values of the lattice parameter of solid solution and values which were found by the Vegard's law, so we obtained the range of possible values of Zn concentrations (Fig. 4) in studied films. These data are presented in Table 1.

As it is seen from Table 1, values of Zn concentration obtained from the XRD data have a good correlation with the values obtained by the EDS method.

Calculation of the values of pole density has shown that films have axial growth texture in [111] direction. It should be noted that the axial growth texture in the [111] direction in II–VI films with zincblende structure is typical for films obtained by the vacuum techniques [13, 18, 22]. Also it was determined that quality of the growth texture in the thin films slightly depends on zinc concentration (Table 2).

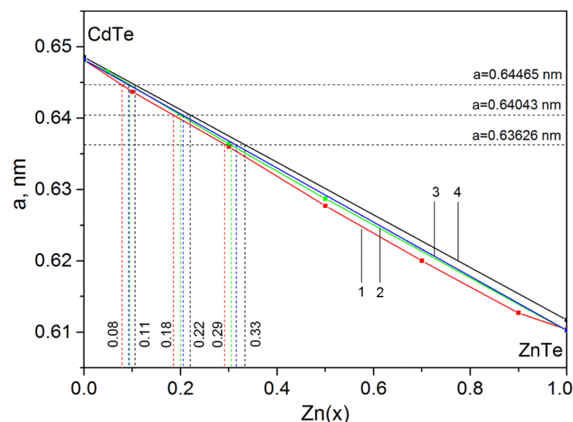


Fig. 4. Determination of zinc concentration in CZT solid solution using lattice parameter (*1* — Berchenko [25], *2* — Ramalingam [26], *3* — Vegard (JCPDS) [15, 24], *4* — our data). Dashed lines show interval of Zn concentration for CZT films according to different reference data.

Results of the calculation of CSD sizes (Eq. 4) and microstrain level (Eq. 5) according to the Debye-Scherrer method in the CZT films in directions perpendicular to (111), (220) and (311) crystallographic planes are shown in Fig. 5. As follows from Fig. 5 the CSD size in (111) direction decreases from 74 to 27 nm with increasing of $x$. A similar trend is observed for all other crystallographic directions. As could be seen from inset of Fig. 5, the microstrain level is increased from 0.0007 to 0.0012 with increasing of zinc concentration from $x = 0$ to $x = 0.09$. On further increasing of zinc con-

Table 3. Microstructural parameters of CdTe, CZT and ZnTe films.

| Sample | Zn($x$) | hkl | $L$, nm Scherrer | $\varepsilon \cdot 10^{-3}$ Scherrer | $L$, nm Gauss | $\varepsilon \cdot 10^{-3}$ Gauss | $L$, nm Cauchy | $\varepsilon \cdot 10^{-3}$ Cauchy |
|---|---|---|---|---|---|---|---|---|
| CdTe | 0 | (111) | 74 | 0.5 | – | – | – | – |
| CZT1 | 0.09 | (111) | 28 | 1.4 | – | – | – | – |
| | | (200) | 41 | 0.9 | – | – | – | – |
| | | (400) | 31 | 1.2 | – | – | – | – |
| | | (200)–400 | – | – | 66 | 1.2 | 49 | 2.1 |
| CZT2 | 0.24 | (111) | 23 | 1.7 | – | – | – | – |
| CZT3 | 0.30 | (111) | 22 | 1.7 | – | – | – | – |
| | | (200) | 38 | 9.5 | – | – | – | – |
| | | (400) | 30 | 1.2 | – | – | – | – |
| | | (200)–400 | – | – | 58 | 1.2 | 45 | 2.1 |
| ZnTe | 1 | (111) | 64 | 0.6 | – | – | – | – |
| | | (222) | 53 | 0.7 | – | – | – | – |
| | | (111)–222 | – | – | 89 | 0.6 | 71 | 1.3 |

centration the microstrain level slowly increases to the value of $\varepsilon_{(111)} = 0.002$.

Also for the samples CZT1, CZT3 and ZnTe the calculation of CSD sizes and microstrain level was performed using more precise method of the Hall approximation. Since only for these samples the peaks of reflection from parallel planes (111)–(222), (200)–(400) were observed on the XRD patterns. Results of the calculation are presented in Table 3. As it is seen from Table 3, CSD sizes calculated using the Debye-Scherrer equation are 1.5–2 times less than results obtained by the Hall approximation. The same tendency is observed in the case of microstrain level calculation. This difference is caused by the fact that, in contrast to Debye-Scherrer method, the Hall approximation method allows to separate the contribution of microstrain and CSD into broadening of the diffraction peak. Therefore, the Hall approximation method is more precise approach.

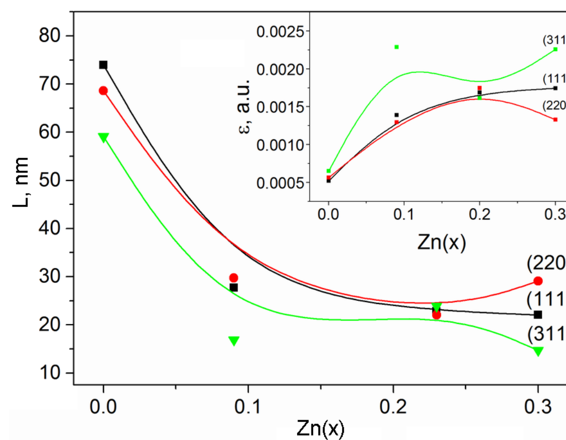


Fig. 5. Dependences of CSD sizes ($L$) of CZT films on zinc concentration. Values for the crystallographic directions [111], [220] and [311] are presented. In the inset dependence of microstrain level ($\varepsilon$) on zinc concentration for the crystallographic directions [111], [220] and [311] is shown.

## 4. Conclusions

In this work polycrystalline films of CdTe, ZnTe compounds and CZT solid solution with variable zinc concentration were obtained by close-spaced vacuum sublimation technique. Optimum grown conditions for deposition of the solid solutions films by the co-evaporation of components were determined, namely temperature of CdTe evaporator $T_{e(CdTe)} = 893$ K, temperature

of ZnTe evaporator $T_{e(ZnTe)}$ = 983 K, substrate temperature $T_s$ = 673 K. The effect of zinc concentration on structural and microstructural properties of the films has been studied. Analysis of surface morphology has shown that obtained films have a polycrystalline structure with the grain size which decreases from 5.0 to 3.5 μm with increasing of zinc concentration. The films were single-phase and contained the cubic phase of CZT. The lattice parameter is decreasing from 0.64947 to 0.63343 nm with zinc concentration increasing. It was determined that with introduction of Zn atoms into CdTe lattice it leads to decreasing in the crystal quality. Namely, the CSD size decreases from 74 nm to 27 nm, and the microstrain level increases from 0.0007 to 0.0022 with increasing of zinc concentration.

## References


1. S.Stolyarova, F.Edelman, A.Chack et al., *J. Phys. D.Appl.Phys.*, **41**, 065402 (2008).
2. H.Xu, R.Xu, J.Huang et al., *Appl.Surf.Sci.*, **305**, 477 (2014).
3. B.Farid, F.Ramaz, O.Panchuk, P.Fochuk et al., *Opt.Mater.(Amst)*, **18**, 7 (2001).
4. K.Yasuda, K.Kojima, K.Mori et al., *J.Electron.Mater.*, **27**, 527 (1998).
5. R.Triboulet, CdTe and Related Compounds; Physics, Defects, Hetero- and Nanostructures, Crystal Growth, Surfaces and Applications: Crystal Growth, Surfaces and Applications, Elsevier (2009).
6. Y.L.Wu, Y.-T.Chen, Z.C.Feng et al., *Hard X-Ray, Gamma-Ray, Neutron Detect.Phys.XI*, **7449**, 74490Q (2009).
7. J.H.Won, K.H.Kim, J.H.Suh et al., *Nucl. Instr. Meth. Phys.Res.A*, **591**, 206 (2008).
8. S.Kang, B.Jung, S.Noh et al., *J.Instrum.*, **7**, C01010 (2012).
9. G.E.Hallani, A.Ryah, N.Hassanain et al., Progress in Electromagnetics Research Symposium Proc. (2011), p.1897.
10. S.H.Lee, A.Gupta, A.D.Compaan, *Phys. Stat. Solidi.*, **1**, 1042 (2004).
11. E.Belas, M.Bugar, R.Grill et al., *J.Electron. Mater.*, **37**, 1212 (2008).
12. D.Nam, H.Cheong, A. Opanasyuk et al., *Phys. Stat. Solidi.*, **4**, 1 (2014).
13. V.Kosyak, A.Opanasyuk, P.Bukivskij, Y.Gnatenko, *J.Cryst.Growth*, **312**, 1726 (2010).
14. J.I.Goldstein, D.E.Newbury, Scanning Electron Microscopy and X-Ray Microanalysis, Plenum Press, New York and London (1981).
15. JCPDS, Intern. Centre for Diffraction Data, USA, Card Number 15-0770.
16. D.K.Bowen, K.B.Tanner, X-Ray Metrology in Semiconductor Manufacturing, Taylor & Francis Group (2006).
17. B.E.Warren, X-ray Diffraction, NY: Dover, Mineola (1990).
18. D.Kurbatov, V.Kosyak, M.Kolesnyk et al., *Integr.Ferroelectr.*, **103**, 32 (2008).
19. S.Lalitha, R.Sathyamoorthy, S.Senthilarasu et al., *Sol.Energy Mater.Sol.Cells*, **82**, 187 (2004).
20. I.P.Kalinkin, Epitaxial Films of II–VI Compounds, LGU, Leningrad (1978) [in Russian].
21. R.Hultgren, P.D.Desai, D.T.Hawkins, Selected Values of the Thermodynamic Properties of Binary Alloys, Metals Park, Amer. Soc. Metals (1973).
22. C.J.Panchal, A.Opanasyuk, V.Kosyak et al., *J. Nano- Electron.Phys.*, **3**, 274 (2011).
23. M.Ivashchenko, A.Opanasyuk, V.Perekrestov et al., *Vacuum*, **119**, 81 (2015).
24. JCPDS, Intern. Centre for Diffraction Data, USA, Card Number 15-0746.
25. N.N.Berchenko, V.E.Krevs, V.G.Seredin, Reference Tables, Voenizdat, Moscow (1982) [in Russian].
26. M.R.Ramalingam, Cadmium Zinc Telluride Solar Cells by Close Spaced Sublimation, University of South Florida (2004).